Available online at www.sciencedirect.com

ScienceDirect

Proceedings of the Combustion Institute 35 (2015) 2233–2240

Proceedings of the Combustion Institute

www.elsevier.com/locate/proci

Kinetics of catalytic oxidation of ethylene over palladium oxide

Y.X. Xin [a], B. Yang [b], H. Wang [c], S.L. Anderson [d], C.K. Law [a,b,*]

[a] Department of Mechanical and Aerospace Engineering, Princeton University, Princeton, NJ 08544, USA
[b] Center for Combustion Energy, Tsinghua University, Beijing 100084, China
[c] Department of Mechanical Engineering, Stanford University, Stanford, CA 94305, USA
[d] Department of Chemistry, University of Utah, Salt Lake City, UT 84112, USA

Available online 10 July 2014

Abstract

Catalytic oxidation of ethylene was experimentally studied by wire microcalorimetry and mass spectrometry over the temperature range of 400–800 K at atmospheric pressure. The catalyst is a palladium oxide (PdO) surface on a polycrystalline palladium wire. For mixtures containing 0.3–0.6% C_2H_4 and 3.75% O_2 in N_2, the heat release rate as well as the mole fractions of gas-phase species were identified. Experimental observation revealed the temperature-dependent channels for the C_2H_4 oxidation, with mixed H_2 release and H_2O production below 580 K and complete oxidation to CO_2 and H_2O above 600 K. Analysis of the global reaction kinetics shows that for $620 \leqslant T\,(\mathrm{K}) \leqslant 740$ K the surface catalytic reaction rate is the first order in ethylene concentration and has an activation energy of 48.2 ± 1.4 kJ/mol. A surface chemistry model is proposed and the dissociative adsorption rate constant of C_2H_4 on PdO surface was determined by fitting the experimental data.

Keywords: Catalytic oxidation; Pd-based catalyst; Ethylene combustion; Surface chemistry

1. Introduction

Increased combustion rates of the products of the endothermic fuel-cooling reactions can be critical to the development of hypersonic engines. During endothermic fuel cooling, hydrogen and several small hydrocarbons, including ethylene (C_2H_4) and methane (CH_4), form before the decomposed products enter the combustor [1]. It was suggested that the combustion of the decomposed products and especially the ignition process may be improved by the use of a freely suspended nanoparticle catalyst [2]. Previously, methane ignition in the presence of palladium (Pd) or palladium oxide (PdO) nanoparticle catalyst has been examined in a flow reactor [2–4]. These studies showed considerable reduction of the ignition delay of methane when Pd nanoparticles are present in the flow. Subsequently, the catalytic oxidation rates of methane, ethane and propane were examined systematically by wire microcalorimetry under

* Corresponding author at: Department of Mechanical and Aerospace Engineering, Princeton University, Princeton, NJ 08544, USA. Fax: +1 (609) 258 6233.
E-mail address: cklaw@princeton.edu (C.K. Law).

http://dx.doi.org/10.1016/j.proci.2014.06.094
1540-7489/

atmospheric pressure [5–7]. Recent work has shown that under certain conditions, wire microcalorimetry can produce fundamental kinetic rate parameters for dissociative-adsorption of the fuel on a PdO surface [6,7].

The oxidation of C_2H_4 on Pd/PdO surfaces has been studied below 600 K. Gas-phase ethylene oxidation over palladium is an industrial process for vinyl acetate synthesis [8]. Over the temperature of 323–413 K, ethylene oxidation over evaporated films of palladium produces carbon dioxide and water directly [9]; and the reaction was zeroth order with respect to oxygen and first order with respect to ethylene at low pressures but evolved to zeroth order at high pressures. Minor products of the reaction include mainly acetic acid and acetate anhydrate. Furthermore, ethylene oxidation over a Pd/γ-Al_2O_3 catalyst at around 600 K [10] was found to have a global activation energy of 13.8 kcal/mol and is inhibited by water in a manner similar to methane oxidation (see, e.g., [11,12]). Studies on the kinetics of vinyl acetate synthesis from ethylene on bulk Pd(1 0 0) and Pd nanoparticles supported on silicate showed quite strong dependence of the reaction rate on the particle size [13].

Studies have also shown that the initial adsorption of ethylene on Pd(1 1 1) surfaces yields a di-σ bond [14,15]. On oxygenated, Pd(1 1 1)2 × 2-O surfaces, both ethylidyne (–CH–CH_3) and a π-bonded configuration are formed at room temperature, but the π-bonded ad-species desorbed completely as the surface is heated [16]. Reaction pathways of C_2H_4 decomposition over PdO surface were investigated recently by density functional theory (DFT) [17–20]. These studies depicted a relatively clear picture of C_2H_4 interaction with Pd surfaces: C_2H_4 adsorbs on the Pd surface followed by the conversion of the ad-species to ethylidyne. Dehydrogenation follows, sequentially converting the ad-species to surface carbon. Under reduced pressure or vacuum-like conditions (a few μbars), the oxidation of ethylene on Pd(1 1 1) surface forms dissolved carbon up to 650 K, above which CO is formed as the main product, along with CO_2 [21,22].

While there is a significant body of work for the catalytic oxidation of C_2H_4 at low temperatures or low pressures, kinetic investigations at high temperatures are clearly needed. Here, we study the catalytic oxidation of ethylene over the surface of polycrystalline palladium by wire microcalorimetry over the temperature range of 400–800 K and under the ambient pressure and dilute fuel concentration. The products were examined by mass spectrometry. The kinetic parameters of C_2H_4 oxidation over Pd were extracted over the temperature range of 620–740 K. The reaction mechanism is discussed along with the rate coefficient of ethylene dissociative adsorption over a PdO surface.

2. Experimental and simulation specifications

2.1. Wire microcalorimetry

Wire microcalorimetry [5–7,23,24] is designed to measure the global heat release rate of surface reactions at a given temperature and gas-phase composition. The experiment is conducted on a metallic wire of catalytic material situated in a quiescent environment. The wire is electrically heated to a certain temperature. The difference in power inputs, Δp, between an inert mixture and a reactive mixture, quantifies the surface heat release rate. For a specific reactive mixture the experiment yields the "ignition" temperature above which a discernible heat production is captured. The Pd wire used was 10 cm long and 0.1 mm in diameter (99.99%, Aldrich), and the gas mixtures of C_2H_4 (99.98%, Airgas), O_2 and N_2 (industrial grade, Airgas) were prepared in a 5.0-L stainless steel cylinder. Four mixtures of 0.3%, 0.4%, 0.5%, 0.6% C_2H_4/3.75% O_2/N_2 by volume, all having equivalence ratios below the flammability limit of 2.7% C_2H_4 under atmosphere pressure, were experimented.

2.2. Mass spectrometry

The concentrations of gas-phase species around the Pd wire were analyzed by an electron ionization mass spectrometer. The apparatus consists of the wire microcalorimetry chamber, a three-stage differentially pumped sampling system, and an RGA 300 mass spectrometer. The schematic of the experimental setup are shown in Fig. S1 in the Supplemental material. The gaseous sample close to the Pd wire (2 mm) was withdrawn through a stainless steel nozzle 0.1 mm in diameter and a 10-cm long inlet tube. The gases exiting the inlet tube then expanded into the first differential region, and the central part of the expansion was collimated by a nickel skimmer (1 mm diameter orifice), passing through the open grids of the mass spectrometer ion source as a molecular beam, and finally passing into a turbomolecular pump. The pressure was around 1×10^{0}, 2×10^{-5} and 1×10^{-7} Torr in the three pumping stages, respectively, and the mass spectrometer was housed in the last stage. All mass spectrometric measurements were carried out with the use of a 70 eV electron energy, and an electron multiplier gain of 1000. The resolution ($\Delta m = 10\%$) is 1 amu and the minimum detectable partial pressure was around 10^{-11} Torr.

2.3. Numerical simulation

To account for possible fluid transport effects on surface reactions, wire microcalorimetry experiment was simulated using FLUENT with surface chemistry. Because of the large ratio of the wire

length over diameter, the simulation was treated as two-dimensional and conducted over the cross section of the wire. The wire was represented as an isothermal wall of surface temperature, T. Ambient temperature, pressure and fresh reactive mixture were applied as the boundary conditions. The length of the simulation domain was chosen to be 70 times the wire diameter, D, which is large enough to ensure that the simulation results are independent of the domain size. Additional details on the computation are given in Ref. [5].

The surface chemistry for the C_2H_4 oxidation over PdO is described by the reaction model given in Table 1, applicable for temperatures above 600 K. This model was largely derived from an earlier study of CH_4 oxidation over PdO [6] (R1-13), with two additional reactions (R14-15) related to ethylene oxidation added. The thermodynamic and transport properties of the gas-phase and surface species are also taken from Ref. [6]. By solving the equations of continuity, momentum, energy and species concentrations, the heat release rate of the surface reactions was simulated and compared to the experimental measurements.

2.4. Surface characterization

Over the temperature range studied, the oxidized state of Pd is thermodynamically favored than the metallic phase [25]. To conduct our experiment in a reproducible manner, the Pd wire was pretreated with a standard procedure [5] that led to the formation of a stable PdO layer at the wire surface. In this procedure, the wire was heated first at 900 K in N_2 for one hour and then exposed to a 2% CH_4/air mixture for another hour. The surface of the treated wire was characterized by Scanning Electron Microscope (SEM) and X-ray Photoelectron Spectroscopy (XPS), showing a 1–2 μm, porous PdO layer over the bulk polycrystalline Pd which remains stable during the oxidation of the ethylene-air mixture. The actual surface area of the porous Pd wire was found to be 3.5 times that of a smooth cylinder [6]. Also, by analyzing the SEM pore distribution, it was found that the pores on the wire surface have a median radius $r = 0.5$ μm and average length $L = 10$ μm.

3. Results and discussion

3.1. Onset temperature of heat release and its rate

Figure 1 presents the heat release rate for the catalytic oxidation of 0.3–0.6% C_2H_4/3.75% O_2/N_2 from 400 to 800 K. Heat release is discernible above an onset temperature of 440 K. Below

Table 1
Surface reaction model of C_2H_4 oxidation.

No.	Reaction[a]	Rate parameters[b]		
		A	β	E
1f	$O_2 + 8Pd(S) \rightarrow 2O^4(S)$	$e^{-T/540-8.8\theta dc}$	0.0	0
1b	$2O^4(S) \rightarrow O_2 + 8Pd(S)$	3.01×10^{26}	−0.5	$230.0–120\theta$[d]
2f	$H(S) + O^4(S) \rightarrow OH^4(S) + Pd(S)$	2.91×10^{18}	1.264	$94.6–60\theta$[d]
2b	$OH^4(S) + Pd(S) \rightarrow H(S) + O^4(S)$	2.29×10^{19}	1.156	$120.3–30\theta$[d]
3f	$H(S) + OH^4(S) \rightarrow H_2O^4(S) + Pd(S)$	6.56×10^{15}	1.403	31.8
3b	$H_2O^4(S) + Pd(S) \rightarrow H(S) + OH^4(S)$	2.11×10^{18}	1.134	$83.8 + 30\theta$[d]
4f	$2OH^4(S) \rightarrow H_2O^4(S) + O^4(S)$	3.89×10^{17}	1.244	$14.5 + 60\theta$[d]
4b	$H_2O^4(S) + O^4(S) \rightarrow 2OH^4(S)$	1.40×10^{19}	1.1	$40.7 + 60\theta$[d]
5f	$H + Pd(S) \rightarrow H(S)$	1.0 [c]	0	0
5b	$H(S) \rightarrow H + Pd(S)$	1.32×10^{10}	1.1	261.7
6f	$O + Pd(S) \rightarrow O^4(S)$	1.0 [c]	0	0
6b	$O^4(S) \rightarrow O + Pd(S)$	1.64×10^{10}	1.1	$369.7–60\theta$[d]
7f	$OH + Pd(S) \rightarrow OH^4(S)$	1.0 [c]	0	0
7b	$OH^4(S) \rightarrow OH + Pd(S)$	1.60×10^{10}	1.1	$227.5–30\theta$[d]
8f	$H_2O + Pd(S) \rightarrow H_2O^4(S)$	1.0 [c]	0	0
8b	$H_2O^4(S) \rightarrow H_2O + Pd(S)$	1.62×10^{10}	1.1	43.8
9	$CO(S) + O^4(S) \rightarrow CO_2 + 5Pd(S)$	1.00×10^{19}	1.115	59.8
10	$C(S) + O^4(S) \rightarrow CO(S) + 4Pd(S)$	1.01×10^{19}	1.115	62.8
11f	$CO + Pd(S) \rightarrow CO(S)$	1.0 [c]	0	0
11b	$CO(S) \rightarrow CO + Pd(S)$	1.65×10^{11}	1.1	134.0
12	$CH_3(S) + 3Pd(S) \rightarrow C(S) + 3H(S)$	1.07×10^{19}	1	85.1
13	$CH_3(S) + 3O^4(S) \rightarrow C(S) + 3OH^4(S)$	1.07×10^{19}	1	25.1
14	$C_2H_4(S) + Pd(S) + O^4(S) \rightarrow CCH_3(S) + OH(S)$	2.5×10^4	0	43.1
15	$CCH_3(s) + O^4(S) \rightarrow CO(s) + CH_3(S)$	1.07×10^{19}	1	25.1

[a] Pd site occupancy of O(S), OH(S) and $H_2O(S)$ is set to 4. Surface site density is 1.95×10^{-9} mol/cm^2.
[b] Rate constant is written in the form $k = AT^{\beta}e^{-E/RT}$. Unit of A are given in terms of mol, cm and s. E is in kJ/mol.
[c] Sticking coefficient.
[d] θ is the total occupied site fraction, i.e., $\theta = 1 - \theta_{Pd}$.

560 K, the heat release rate is seen to be independent of temperature and only mildly dependent on the ethylene concentration. The observation is in agreement with the previous observation of C_2H_4 oxidation on a Pd film [9], in which the reaction was found to be of zeroth order with respect to C_2H_4 under similar conditions. The cause for the plateau is the limited number of surface sites for C_2H_4 adsorption and dehydrogenation because the surface is expected to be fully oxidized over this temperature range. Above 560 K, the heat release rate increases with the surface temperature and becomes a function of the C_2H_4 concentration.

3.2. Species produced from catalytic processes

To explore the reaction pathways and identify the products, species were extracted at a position 2 mm from the wire with the sampling rate around 1 cm^3/s and analyzed by a mass spectrometer for experiments using a mixture containing 0.5% C_2H_4/3.75% O_2/1% He/Ar. The chosen sampling position was a compromise between maximizing the species signal and the minimizing the sampling effect on the surface reaction. Helium was used as the internal standard and N_2 was replaced by Ar because of its interference with the crucial peak at $m/z = 28$; recognizing nevertheless that a trace amount of N_2 was always present in the system. The measurement was performed over the temperature range of 400–800 K. The spectrum generated was normalized by the intensity of the He peak ($m/z = 4$). The reproducibility of the normalized intensities is within ±5%.

Figure 2 shows a sample mass spectrum recorded at 600 K. The peaks at $m/z = 14$, 27, 28 have major contributions from ionization and dissociative ionization of C_2H_4; those at $m/z = 14$, 28 also have contributions from N_2, those at $m/z = 28$, 44 from CO_2 and those at $m/z = 20$ and 40 result from Ar^{2+} and Ar^{+}. The peak around m/z = 36 comes from the isotope of Ar. Since no notable peaks with m/z above 44 were observed, there is no evidence to confirm the presence of acetic acid or acetate anhydride as the major products of the current catalytic experiments. To discern the level of CO produced from catalytic experiments, the peak at $m/z = 28$ was analyzed in detail. Specifically, spectra of pure C_2H_4, N_2, and CO_2 were measured and adopted as the internal standard. Calibration was also made using a mixture containing 5% CO and 5% CO_2 diluted in a mixture of Ar and He. Each spectrum collected under the catalytic reaction condition was processed to subtract the collective contributions from C_2H_4, N_2 and CO_2 at $m/z = 28$ by considering the intensities at $m/z = 27$, 14 and 44, respectively. Figure 3 plots the residual signal intensities at $m/z = 28$. It is seen that there is no discernible correlation between the residue intensity and temperature. Based on this observation, it is concluded that the level of CO is below the background noise. The upper limit of the CO/CO_2 ratio may be estimated by assuming the residual signal intensity at $m/z = 28$ to be solely from CO. The maximum CO/CO_2 ratio is smaller than 10% at 400 K owing to the weak signal of CO_2, and zero at higher temperatures.

The mole percentages of the species measured are shown in Fig. 4. At 400 K, appreciable amounts of CO, H_2 and H_2O were measured even though the heat release rate is below the sensitivity of wire microcalorimetry. Towards the high temperatures, the dominant product is CO_2, followed by H_2. The carbon balance is excellent as seen in Fig. 5, which confirms that CO_2 is the dominant product at 800 K. The missing hydrogen and oxygen from the elemental balance at 700 and 800 K is caused by water condensation in the sampling line. Two pieces of evidence support this assertion. First, the missing hydrogen is almost exactly two times the missing oxygen. Second, when the actual H_2O mole percentage is inferred from the missing hydrogen and the as-measured H_2O data of Fig. 4,

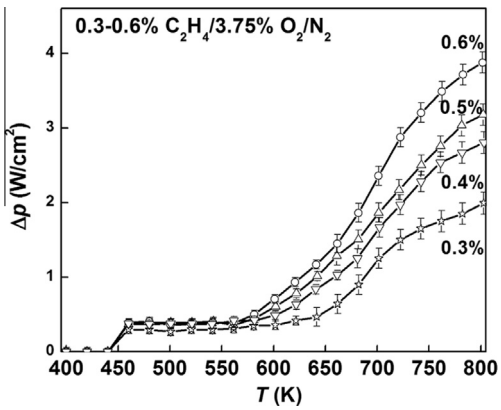

Fig. 1. Heat release rates observed for the oxidation of $C_2H_4/O_2/N_2$ mixtures over a PdO surface. Symbols are experimental data; lines are drawn to guide the eye.

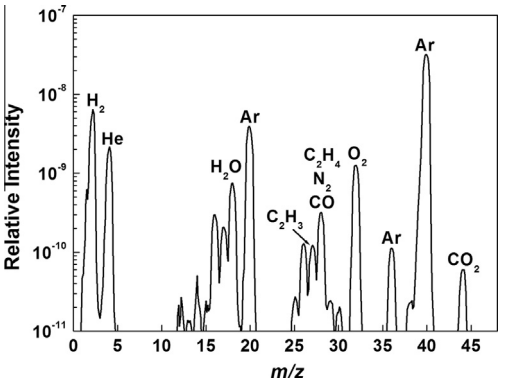

Fig. 2. A typical mass spectrum of gas sampled at 600 K.

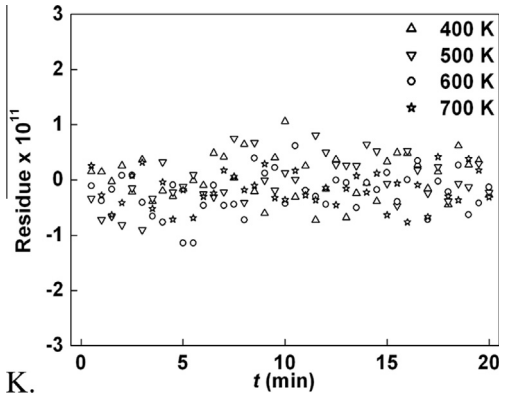

Fig. 3. Residual peak intensities at $m/z = 28$. Mean residue values are 5×10^{-13} at 400 K, -2×10^{-13} at 500 K, and -2×10^{-12} at 600 and 700 K.

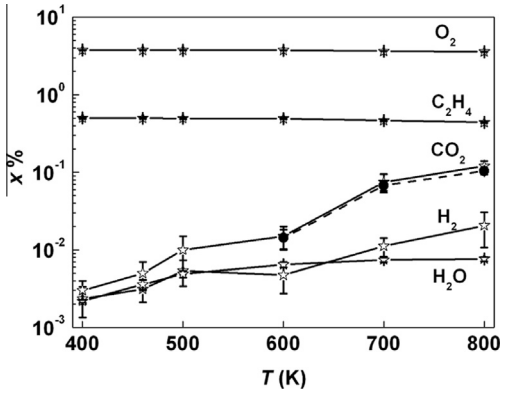

Fig. 4. Mole percentage of major species C_2H_4, O_2, CO_2, H_2 and H_2O sampled near the wire surface. Symbols are experimental data; solid lines are drawn to guide the eye. The solid circle and dashed line indicates the mole percentages of water inferred from the missing hydrogen element above 600 K (see text).

the mole percentage of H_2O follows closely that of CO_2 at and above 600 K, as shown by the solid circle and dashed line in the same figure. Therefore, the analysis suggests that the surface reactions yield predominantly CO_2 and H_2O above 600 K. Below 600 K, both H_2 and H_2O are produced and their concentrations can be similar. In fact, the temperature at which H_2O dominates over H_2 coincides with the onset temperature of rapid heat release beyond the plateau regime, as seen in Fig. 1.

3.3. Surface reaction mechanism and kinetic parameters

The MS analysis just discussed suggests that above 600 K the surface reaction produces predominantly CO_2 and H_2O. Here we extended our early global kinetic analysis for methane,

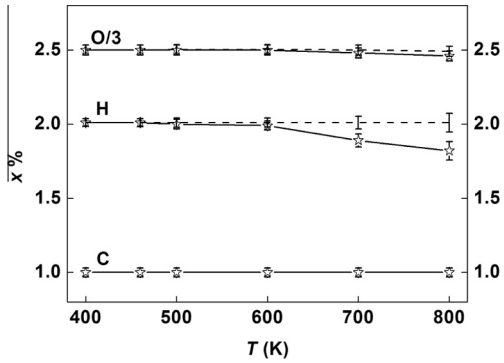

Fig. 5. Mole percentage of H, O, C elements in gas sampled. Symbols are experimental data; solid lines are drawn to guide the eye. The dashed lines indicate inferred mass conservation if all missing H element is attributed to H_2O (see text).

ethane, and propane oxidation to ethylene. Specifically, the apparent rate constant k_{app} and the reaction order with respect to ethylene, n, were extracted from the measured heat release rate using [6].

$$\omega_{app} = \frac{\Delta p}{3.5 \Delta H_r(T)} = k_{app} c^n$$

where ω_{app} is the apparent reaction rate, ΔH_r the lower heating value of ethylene (J/mol), and c the molar concentration of ethylene in the free stream. A plot of ω_{app} as a function of c, shown in Fig. 6, yields k_{app} as the intercept and n as the slope. Figure 7 plots the resulting n value as a function of temperature. Clearly the current experiment indicates that the reaction order is unity with respect to ethylene concentration, a conclusion identical to our earlier studies on methane [6], ethane and propane [7].

The apparent reaction rate coefficient k_{app} corresponding to a unity reaction order is shown as an Arrhenius plot in Fig. 8 and can be expressed by

$$k_{app}(\mathrm{cm/s}) = (1.9 \pm 0.1) \times 10^4 \times \exp\left[-\frac{48.2 \pm 1.4\ \mathrm{kJ/mol}}{RT}\right]$$

over the temperature range of 620–740 K. Keeping in mind that the ΔH_r value used does not consider H_2 as a minor product, the above expression probably represents the upper limit for ethylene oxidation over a Pd surface. In comparison, the apparent activation energies are 62.3, 57.6 and 48.2 kJ/mol for methane, ethane and propane, respectively, under comparable conditions [7]. Clearly the reactivity of ethylene is closer to propane than to methane.

The apparent rate coefficient is shown to level off above 740 K – a phenomenon frequently

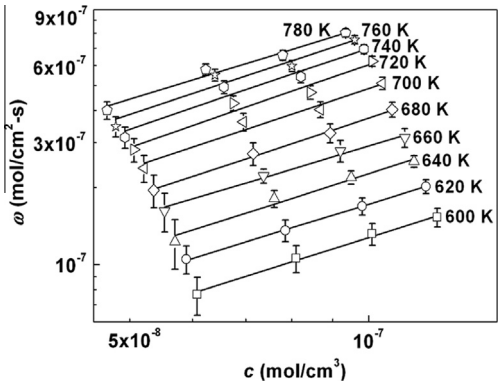

Fig. 6. Apparent reaction rates as a function of molar concentration of ethylene observed for the oxidation of 0.3–0.6% C_2H_4/3.75% O_2/N_2 mixtures over a PdO surface. Symbols are experimental data; lines are fits to data, where the slopes yield the values of the reaction order with respect to C_2H_4 concentration.

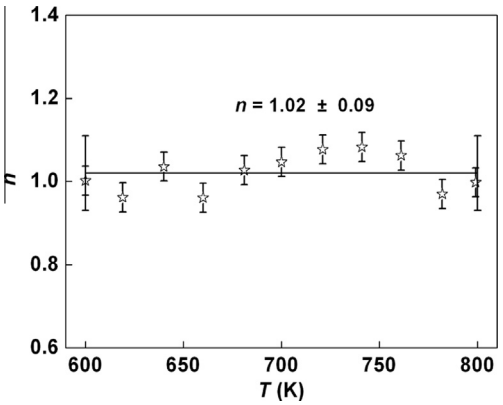

Fig. 7. Overall reaction order with respect to C_2H_4 over a PdO surface. Symbols are experimental data; line represents the average over 600–780 K.

observed for hydrocarbon oxidation over Pd-based catalyst [6,7,26–29]. This observation is attributed, to a large extent, to diffusion limitation and possibly changes in the surface chemistry. To illustrate the diffusional limitation, the impact of diffusion was analyzed by calculating the Thiele modulus [30] as $h_T = \sqrt{2k_{app}L^2/(rD)}$, where D is diffusivity of the reactant, and r and L characterize the geometrical properties of the pore configuration. At 800 K, k_{app} is 13.50 cm/s, obtained by extrapolating the apparent rate constant of Fig. 8 to that temperature, and D is 1.08 cm^2/s for C_2H_4 in the 0.5% C_2H_4/3.75% O_2/N_2, calculated using a mixture-averaged model and transport data of the CHEMKIN package [31]. The Thiele modulus h_T was found to be 0.71. The corresponding effectiveness factor follows the definition of the classical Thiele modulus as

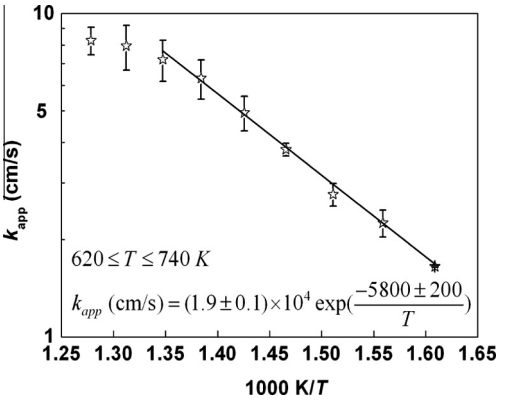

Fig. 8. Apparent rate coefficients for the oxidation of 0.3–0.6% C_2H_4/3.75% O_2/N_2 over a PdO surface from 600 to 740 K. Symbols are experimental data; the line is the Arrhenius fit to the data.

$\eta = \tanh h_T/h_T$, and is calculated as 0.86, which clearly suggests that diffusion limitation plays an important role at that temperature, compared to the typical diffusion-limited threshold of $\eta < 0.95$. Furthermore, the η value is 0.94 at 700 K, indicating a drastically reduced pore diffusion effect below that temperature.

It is noted that no direct and detailed mechanistic information about CO_2 and H_2O production can be deduced from the current experiment. Previously, we showed that under the condition of wire microcalorimetry, the overall rate of catalytic reaction over Pd is sensitive to only two reaction steps: the adsorption and desorption of oxygen and the dissociative adsorption of hydrocarbon [6,7]. If this is also true for ethylene, an exact knowledge of the surface reaction steps is not critical to a prediction of the overall reaction rate. Here we postulate that the initial reaction of ethylene with a PdO surface may be described reaction R14 and R15 of Table 1. Along with other reaction steps proposed for methane oxidation [6], we find the value of k_{14} iteratively by fitting the microcalorimetry data at each temperature and gas composition. The results are shown in Fig 9 and are fitted to an Arrhenius expression:

$$k_{14}(\mathrm{cm/s}) = (2.5 \pm 0.1) \times 10^4 \exp\left[-\frac{43.1 \pm 0.8\ \mathrm{kJ/mol}}{RT}\right]$$

over the temperature range of 620–740 K. Sensitivity analysis was performed again identifying the adsorption/desorption of O_2 and the dissociative adsorption of C_2H_4 to be the critical reaction steps. Compared to the activation energies of methane, ethane and propane oxidation under comparable conditions (58, 53 and 44 kJ/mol, respectively) [7], the activation energy of ethylene dissociative adsorption is the lowest. The pre-exponent factor lies between those of ethane (4.5×10^4 cm/s) and propane (1.6×10^4 cm/s).

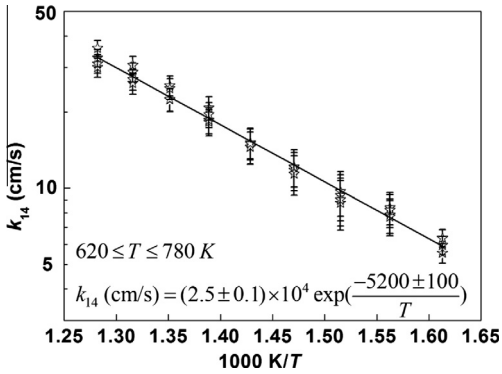

Fig. 9. Rate coefficients of C_2H_4 adsorption over PdO surface for mixtures of 0.3–0.6% C_2H_4/3.75% O_2/N_2. Symbols are derived by fitting the wire microcalorimetry data through detailed modeling; the line is an Arrhenius fit to the data.

Below 600 K, C_2H_4 undergoes dehydrogenation reaction on the PdO surface in addition to H_2O production. No detailed analysis is conducted here because of the detailed reaction mechanism needed to describe the overall heat release rate is currently unavailable. In any case, the temperature regime is too low to have any practical implication for combustion applications.

4. Conclusions

Catalytic oxidation of 0.3–0.6%C_2H_4/3.75%O_2/N_2 mixtures was studied over PdO surface by wire microcalorimetry and mass spectrometry over the temperature range of 400–800 K and under atmospheric pressure. Heat release was observed starting from 450 K. From this temperature and below 580 K, the heat release rate was found to be independent of temperature and only mildly dependent on the ethylene concentration. The primary reaction products include CO_2, H_2 and H_2O. Above 580 K, the heat release rate increases drastically as a function of temperature and the primary reaction products are CO_2 and H_2O. The heat release rates were analyzed, which yielded a global activation energy of 48.2 ± 2.5 kJ/mol and a reaction order of unity over the temperature of 620–740 K. A surface chemistry model was proposed for reaction over 620–740 K. The rate coefficient of ethylene dissociative adsorption on Pd surface was proposed by fitting the microcalorimetry data.

Acknowledgements

The authors acknowledge support by the Air Force Office of Scientific Research through a MURI program FA9550-08-1-0400, Nanocatalysts in Propulsion under the technical monitoring of Dr. Michael R. Berman. Bin Yang is also grateful to the support of Natural Science Foundation of China (51306102).

Appendix A. Supplementary data

Supplementary data associated with this article can be found, in the online version, at http://dx.doi.org/10.1016/j.proci.2014.06.094.

References

[1] M.B. Colket, L.J. Spadaccini, *J. Propul. Power* 17 (2) (2001) 315–323.
[2] T. Shimizu, A.D. Abid, G. Poskrebyshev, et al., *Combust. Flame* 157 (3) (2010) 421–435.
[3] B. Van Devener, S.L. Anderson, T. Shimizu, et al., *J. Phys. Chem.* 113 (48) (2009) 20632–20639.
[4] T. Shimizu, H. Wang, *Proc. Combust. Inst.* 33 (2011) 1859–1866.
[5] T.C. Zhang, Y.X. Xin, Z.Y. Ren, F. Qi, C.K. Law, *Combust. Flame* 160 (1) (2013) 149–154.
[6] Y.X. Xin, S. Lieb, H. Wang, C.K. Law, *J. Phys. Chem. C* 117 (38) (2013) 19499–19507.
[7] Y.X. Xin, H. Wang, C.K. Law, *Combust. Flame* 161 (4) (2014) 1048–1054.
[8] M.G. Clerici, M. Ricci, G. Strukul, in: G.P. Chiusoli, P.M. Maitlis (Eds.), *Metal-catalysis in Industrial Organic Processes*, Royal Society of Chemistry, Cambridge, 2008, p. 23.
[9] C. Kemball, W.R. Patterson, *Proc. R. Soc. London, A* 270 (1341) (1962) 219–231.
[10] L. van de Beld, M.C. van der Ven, K.R. Westerterp, *Chem. Eng. Proc.* 34 (5) (1995) 469–478.
[11] D. Ciuparu, L. Pfefferle, *Appl. Catal., A* 209 (1–2) (2001) 415–428.
[12] K. Persson, L.D. Pfefferle, W. Schwartz, A. Ersson, S.G. Jaras, *Appl. Catal., B* 74 (3–4) (2007) 242–250.
[13] D. Kumar, Y.F. Han, D.W. Goodman, *Catal. Lett.* 106 (1–2) (2006) 1–5.
[14] L.L. Kesmodel, J.A. Gates, *Surf. Sci.* 111 (3) (1981) L747–754.
[15] M. Kaltchev, A.W. Thompson, W.T. Tysoe, *Surf. Sci.* 391 (1–3) (1997) 145–149.
[16] M. Sock, A. Eichler, S. Surnev, J.N. Andersen, B. Klotzer, K. Hayek, M.G. Ramsey, F.P. Netzer, *Surf. Sci.* 545 (1–2) (2003) 122–136.
[17] Z.X. Chen, H.A. Aleksandrov, D. Basaran, N. Rosch, *J. Phys. Chem. C* 114 (1) (2010) 17683–17692.
[18] D. Basarana, H.A. Aleksandrova, Z.X. Chen, Z.J. Zhao, N. Rosch, *J. Mol. Catal. A: Chem.* 344 (1–2) (2011) 37–46.
[19] J. Andersin, N. Lopez, K. Honkala, *J. Phys. Chem. C* 113 (19) (2009) 8278–8286.
[20] J. Andersin, K. Honkala, *Surf. Sci.* 604 (9–10) (2010) 762–769.
[21] H. Gabasch, K. Hayek, B. Klotzer, A. Knop-Gericke, R. Schlogl, *J. Phys. Chem. B* 110 (10) (2006) 4947–4952.

[22] H. Gabasch, A. Knop-Gericke, R. Schlogl, W. Unterberger, K. Hayek, B. Klotzer, *Catal. Lett.* 119 (3–4) (2007) 191–198.
[23] L. Hiam, H. Wise, S. Chaikin, *J. Catal.* 10 (3) (1968) 272–276.
[24] P. Cho, C.K. Law, *Combust. Flame* 66 (2) (1986) 159–170.
[25] C. Mallika, O.M. Sreedharan, J.B. Gnanamoorthy, *J. Less Common Met.* 95 (2) (1983) 213–220.
[26] T. Engel, *J. Chem. Phys.* 69 (1) (1978) 373–385.
[27] J.G. McCarty, *Catal. Today* 26 (3–4) (1995) 283–293.
[28] R.J. Farrauto, M.C. Hobson, T. Kennelly, E.M. Waterman, *Appl. Catal., A* 81 (2) (1992) 227–237.
[29] A.K. Datye, J. Bravo, T.R. Nelson, P. Atanasova, M. Lyubovsky, L. Pfefferle, *Appl. Catal., A* 198 (1–2) (2000) 179–196.
[30] C.G. Hill, *An Introduction to Chemical Engineering Kinetics and Reactor Design*, John Wiley and Sons Inc, New York, U.S., 1977, p. 220.
[31] R.J. Kee, F.M. Rupley, J.A. Miller, et al., *CHEMKIN Collection, Release 2.2*, Reaction Design, Inc., San Diego, CA, 2000.